Plant Physiology and Biochemistry 208 (2024) 108483

Contents lists available at ScienceDirect

Plant Physiology and Biochemistry

journal homepage: www.elsevier.com/locate/plaphy

Interplay between secondary metabolites and plant hormones in silver nitrate-elicited *Arabidopsis thaliana* plants

Eva Cañizares, Juan Manuel Acién, Berivan Özlem Gumuş, Vicente Vives-Peris, Miguel González-Guzmán **, Vicent Arbona *

Dept. Biologia, Bioquímica I Ciències Naturals, Universitat Jaume I, Castelló de La Plana, Spain

ARTICLE INFO

Keywords:
Arabidopsis
Glucosinolates
Metabolomics
Methyl jasmonate
Salicylic acid
Signaling
Transcription factor

ABSTRACT

Plants produce a myriad of specialized compounds in response to threats such as pathogens or pests and different abiotic factors. The stress-related induction of specialized metabolites can be mimicked using silver nitrate ($AgNO_3$) as an elicitor, which application in conservation agriculture has gained interest. In *Arabidopsis thaliana*, $AgNO_3$ triggers the accumulation of indole glucosinolates (IGs) and the phytoalexin camalexin as well as pheylpropanoid-derived defensive metabolites such as coumaroylagmatins and scopoletin through a yet unknown mechanism. In this work, the role of jasmonic (JA) and salicylic acid (SA) signaling in the $AgNO_3$-triggered specialized metabolite production was investigated. To attain this objective, $AgNO_3$, MeJA and SA were applied to *A. thaliana* lines impaired in JA or SA signaling, or affected in the endogenous levels of IGs and AGs. Metabolomics data indicated that $AgNO_3$ elicitation required an intact JA and SA signaling to elicit the metabolic response, although mutants impaired in hormone signaling retained certain capacity to induce specialized metabolites. In turn, plants overproducing or abolishing IGs production had also an altered hormonal signaling response, both in the accumulation of signaling molecules and the molecular response mechanisms (ORA59, PDF1.2, VSP2 and PR1 gene expression), which pointed out to a crosstalk between defense hormones and specialized metabolites. The present work provides evidence of a crosstalk mechanism between JA and SA underlying $AgNO_3$ defense metabolite elicitation in *A. thaliana*. In this mechanism, IGs would act as retrograde feedback signals dampening the hormonal response; hence, expanding the signaling molecule concept.

1. Introduction

Plant species are highly diverse in the array of specialized metabolites they synthesize, some of them can be highly specific of family and even genus. These specialized metabolites are important in the adaptation of plants to their surrounding environment and have several biological activities such as UV screen, antioxidants, attractants of pest predators or parasitoids, emergency signals for other plants of the same or different species, communication with other organisms in the phyllosphere or rhizosphere, pest deterrents or repellers or even as toxic compounds (Erb and Kliebenstein, 2020). In the model plant *Arabidopsis thaliana*, the most abundant compounds are glucosinolates, a class of compounds harboring a β-thioglucosyl residue attached to an α-carbon constituting a sulfated ketoxime, deriving from amino acids Met, Ala, Val, Leu or Ile, Phe or Tyr and Trp (Grubb and Abel, 2006). Intact glucosinolates are quite stable and can be metabolized by myrosinases, a specific class of thioglucosidases, releasing several classes of highly reactive and toxic compounds: isothiocyanates, nitriles, thiocyanates, oxazolidine-2-thiones or epithionitriles. Moreover, Arabidopsis also synthesizes the indolic phytoalexin camalexin arising from Trp, an abundant specialized metabolite in this plant species (Ahuja et al., 2012; Böttcher et al., 2009).

The production of these compounds is regulated by complex molecular mechanisms involving several members of the MYB family of transcription factors (TF). Using an expression activation-tagging strategy, (Gigolashvili et al., 2007) identified the R2R3-MYB TF gene HIGH INDOLIC GLUCOSINOLATE 1 (HIG1) or MYB51 which transactivates promoters of genes involved in indolic glucosinolate (IG) biosynthesis in Arabidopsis: TSB1 (involved in tryptophan biosynthesis), CYP79B2 and CYP79B3 (a metabolic hub in indolic compound biosynthesis, including

* Corresponding author.
** Co-corresponding authors.
E-mail addresses: mguzman@uji.es (M. González-Guzmán), arbona@uji.es (V. Arbona).

https://doi.org/10.1016/j.plaphy.2024.108483
Received 31 October 2023; Received in revised form 23 February 2024; Accepted 29 February 2024
Available online 1 March 2024

indole-3-acetic acid, indole glucosinolates and camalexin), CYP83B1 (or SUR2) and the sulfotransferase ST5α. The overexpression of ATR1 (MYB34) also resulted in enhanced indole glucosinolate and indole-3-acetic acid levels (Gigolashvili et al., 2007). Following a similar approach, (Sønderby et al., 2007) identified MYB28 as a key regulator of aliphatic glucosinolate biosynthesis along with its homologues MYB29 and MYB76. Hence, MYB28 and MYB29 are primarily involved in the regulation of the biosynthesis of aliphatic glucosinolates (AG) and have been associated to the induction of CYP79F1 and CYP79F2 which catalyze the formation of the alkyl aldoxime; CYP83A1, which catalyzes the formation of the S-alkyl-thiohydroxymate and the sulfotransferases SOT17 and SOT18 which render the final product (Grubb and Abel, 2006). In the IG branch, other MYB factors such as MYB122 are involved, inducing similar steps within the indole biosynthetic pathway (Kim et al., 2008).

Apart from glucosinolates, Arabidopsis also synthesizes other specialized metabolites such as phenylpropanoids and flavonoids which biosynthesis is also regulated by a group of MYB transcription factors (MYB4, MYB12 and MYB75/PAP1) (Jogawat et al., 2021; Liu et al., 2015). The overexpression of some of these MYBs has an impact on flavonoid accumulation by targeting biosynthetic genes such as those encoding chalcone synthase (CHS) and chalcone isomerase (CHI), flavanone-3-hydroxylase (F3H), flavonol synthase (FLS) and dihydroflavonol reductase (DFR) (Nakabayashi et al., 2014). Phenylpropanoids derive from the phenylalanine ammonia lyase (PAL) pathway leading to the synthesis of phenolic acids and conjugates (with polyamines, carbohydrates, or other compounds), building blocks in lignin biosynthesis, flavonoids (*via* the CHS and CHI pathway) (Böttcher et al., 2008). Phenylpropanoids and flavonoids are known to act as scavengers of reactive oxygen species (ROS) and as UVB light screen. Moreover, their involvement in ROS-dependent secondary root growth in Arabidopsis has also been shown (Silva-Navas et al., 2016).

Plant hormones such as salicylic acid (SA) and jasmonates (JAs) integrate exogenous cues with the biosynthesis of different specialized compounds (Jogawat et al., 2021). SA derives from chorismate through the PAL/BA2H pathway or through isochorismate *via* the isochorismate synthase 2 (ICS2) pathway (Lefevere et al., 2020). This plant hormone binds the endogenous SA receptor NON-PATHOGENESIS RELATED 1 (NPR1) triggering the expression of PATHOGENESIS-RELATED 1 (PR1) and specialized metabolite biosynthesis (Durango et al., 2013; Zhang et al., 2020). JAs are synthesized from membrane lipids through the lipoxygenase 3 (LOX3) pathway (Wasternack, 2007). The active signaling molecule of jasmonates is jasmonoyl-isoleucine (JA-Ile) which is synthesized in the cell cytoplasm by conjugating jasmonic acid (JA) to an isoleucine moiety. JA-Ile binds to its receptor COI1 which, in turn, activates a COI1-dependent ubiquitin E3-ligase that targets JAZs (JAsmonate Zim-domain proteins) transcriptional repressors for proteasomal degradation. Their degradation releases JA-dependent gene expression *via* ERF1 and MYC2 TFs (Chini et al., 2009), which in turn regulate the expression of defensins PDF1.2 and VSP2, respectively (Fernández-Calvo et al., 2011; Zarate et al., 2007). Indeed, JA signaling seems to be essential for triggering metabolic defenses of *Arabidopsis thaliana* against phytophagous spider mites (Widemann et al., 2021; Zhurov et al., 2014). Moreover, it has been reported that Col-0 accumulates primarily IGs in response to MeJA *via* multiple pathways leading to the build-up of indol-3-methyl and 1-methoxyindol-3-ylmethyl glucosinolates, whereas SA treatment increases 4-Methoxyindol-3-ylmethyl glucosinolate concentration (Kliebenstein et al., 2002).

The specialized metabolite response induced by stimuli such as herbivores, pathogens, hormones, and other abiotic factors can be mimicked by the application of exogenous treatments such as inorganic chemicals or pathogen-derived molecules (Liu et al., 2022). To this respect, the most powerful and widely known chemical treatment is $AgNO_3$ (Yoshikawa, 1978), which has been shown to be effective elicitating plant specialized metabolite responses in different plant species (Böttcher et al., 2009; Cessur et al., 2023; Kruszka et al., 2020; Moesta and Grisebach, 1980; Wei et al., 2022). Moreover, when it is applied as metal nanoparticles (AgNPs), it shows better physico-chemical properties than its respective bulk material or ionic forms (Kruszka et al., 2020). However, $AgNO_3$ is a well-known hazardous and pollutant chemical compound and both $AgNO_3$ and AgNPs act as toxic compounds in plants reducing growth and inducing the accumulation of ROS in plant tissues (Vishwakarma et al., 2017). Despite its toxicity, $AgNO_3$ has been used in plant experimentation to elicit specialized metabolite biosynthesis in Arabidopsis (Böttcher et al., 2009; Glawischnig et al., 2004; Schuhegger et al., 2006) or to promote the *in vitro* shoot development and plant regeneration in different plant species (Hyde and Phillips, 1996; Venkatachalam et al., 2017). However, the specific mode of action of $AgNO_3$ in inducing different specialized metabolite accumulation is not clearly understood.

Therefore, to investigate the role of the SA and JA-dependent hormonal signaling and their putative crosstalk in the $AgNO_3$-induced accumulation of different specialized metabolites in *Arabidopsis thaliana*, an approach involving different biosynthetic and signaling mutants of Arabidopsis was employed. Samples were treated with methyl JA (MeJA), SA or $AgNO_3$ and the metabolite profiles and relevant gene expression analyzed.

Table 1
List of Arabidopsis mutants used in the experiments described in this manuscript.

Mutant ID	Locus/loci	Phenotype	References
npr1-2	AT1G64280	Deficient in the SA receptor NPR1, unable to mount typical SA-dependent responses.	Cao et al. (1997)
coi1-16	AT2G39940	Partially insensitive to MeJA and coronatine, susceptible to oomycetes.	Ellis and Turner (2002)
atr1D	AT5G60890	Deregulated tryptophan and IG biosynthesis	Bender and Fink (1998) Celenza et al. (2005)
cyp79b2/ cyp79b3	AT4G39950 AT2G22330	Unable to synthesize IGs or camalexin	Zhao et al. (2002)
myb28/myb29	AT5G61420 AT5G07690	Unable to synthesize AGs	Sønderby et al. (2007)
myb29/myb28/ cyp79b2/ cyp79b3 (qKO)	AT5G61420 AT5G07690 AT4G39950 AT2G22330	Unable to synthesize IGs or AGs	Sønderby et al. (2007)

2. Materials and methods

2.1. Plant material and treatments

Seeds of *Arabidopsis thaliana* of the genotypes listed in Table 1 were individually sown in jiffy pellets (Jiffy Products España, SLU, Murcia, Spain). Seedlings were allowed to grow for six weeks in growth chambers under the following conditions: 8/16 h light/dark cycle and 21 °C/18 °C day/night temperatures, relative humidity at 70% and light intensity at 130 μmol m^{-2} s^{-1} (measured at plant rosette height). After the growth period, plants were randomly distributed into groups and treated with 5 mM $AgNO_3$ (Böttcher et al., 2009), 0.5 mM MeJA or 0.1 mM SA (Venegas-Molina et al., 2020) by spraying a fine mist on rosettes (3 biological replicates, 4 plants per biological replicate). A mock control treatment was established by spraying plants with distilled water. After spraying, plants were again maintained under the same conditions for another 24 h and, subsequently, whole rosettes were harvested, frozen in liquid nitrogen, and crushed to a fine powder.

2.2. Extraction of plant material for metabolomics

Extraction of plant material was carried out as in a previous study

(De Ollas et al., 2021). Briefly, powdered frozen tissue (~50 mg, the actual weight was recorded) was extracted in 80% aqueous methanol (400 μL, LC/MS grade) supplemented with biochanin A as internal standard at 1 mg L^{-1} concentration by ultrasonication for 10 min at room temperature. Extracts were centrifuged at 10,000 rpm for 10 min at 4 °C and the supernatant recovered and filtered through 0.2 μm PTFE syringe filters. The filtered extracts were collected in amber glass chromatography vials with screw caps and pre-slit PTFE septa, properly labeled and immediately analyzed.

2.3. Analytical conditions for metabolomics

Separation of extracts was achieved by reversed phase liquid chromatography on a C18 column (Luna Omega C18 Polar 1.7 μm 100 × 2.2 mm, Phenomenex, CA, USA) using ultrapure water (A) and acetonitrile (B, LC/MS grade) as solvents, both supplemented with formic acid at 0.1 % (v/v). A linear gradient was established starting from 95% A to 5% B (0–2 min) to reach 5% A and 95% in 14 min. During runs, solvent flow rate was kept constant at 0.3 mL min^{-1} and column temperature at 40 °C. Samples were maintained at 10 °C to delay sample decay. Acquisition of mass data was performed in both positive (ESI+) and negative (ESI-) electrospray ionization modes in a Xevo Synapt XS system (Micromass Ltd., UK). The conditions used were as follows: 30 V sampling cone, 4.7 L M resolution, 15.0 H M resolution, 2.0 pre-filter, 1.0 ion energy, 4.0 trap collision energy and 2.0 transfer collision energy; each mode only differing in capillary voltage, 1.73 kV for ESI+ and 1.5 kV for ESI-. Mass data was acquired within the 50–1000 amu scan range setting two functions working at the same time 1) one with low-collision induced dissociation (collision energy set at 10 eV for parent survey) and 2) one with high-collision induced dissociation (setting a ramp for product scanning between 10 and 40 eV). Both functions were acquired and processed independently. A third function to scan the lockmass signal (leucine enkephalin, $[M+H]^+$ 556.2925 and $[M-H]^-$ 554.2745) was also set and mass spectra continuously acquired during runs with the dual spray option, allowing for the correction of mass values of detected compounds.

2.4. Processing of metabolomics data

Raw mass chromatograms (only function 1) were converted to mzML using the msconvert tool from the Proteowizard package (Chambers et al., 2012). Then, the resulting files were grouped into folders according to sample treatment. Chromatograms were subsequently processed using the software xcms (Smith et al., 2006) which performs automatic mass chromatogram peak picking, alignment and retention time corrections. Compound spectra extraction and annotation was performed with the CAMERA package (Kuhl et al., 2012). The resulting datasets were normalized to internal standard peak area (biochanin A, $[M+H]^+$ 285.07, $[M-H]^-$ 283.06) for each chromatographic run and to actual sample weight. Compound identification was attained first by identification of suitable candidates through interrogation of public databases (Human Metabolome Database and Massbank) with potential parent ions ($[M+H]^+$ or $[M-H]^-$). Metabolite annotation was carried out by querying curated experimental mass spectra in public spectral libraries. When a potential positive match was identified, it was confirmed by co-injecting a standard sample of the candidate metabolite using the same chromatographic and mass spectrometry conditions (level 1 annotation). However, when no standard was available, metabolites were tentatively annotated (level 2 annotation) by comparing both experimental and library-curated mass spectra. Finally, when no mass spectra library was available, but a potential identity was found, experimental mass spectrum was manually justified using Chemdraw software (CambridgeSoft, UK) and its *in silico* mass fragmentation function (level 3 annotation).

Table 2
List of genes involved in glucosinolate, flavonoid and phenylpropanoid biosynthesis, SA and JA signaling.

Gene	AGI code	Description	Function	Reference
PR1	At2g14610	Pathogenesis-related protein 1	Pathogens and SA signaling/response	Payne et al. (1988)
ORA59	At1g06160	ERF/AP2 transcription factor family	JA signaling/ response (ERF1 pathway)	Pré et al. (2008)
PDF1.2	At3g23240	Defensin-like protein 16	Ethylene and JA signaling/ response, defense	Penninckx et al. (1996)
VSP2	At5g24770	Vegetative storage protein 2	Insect and JA (MYC2 pathway) signaling/response	Utsugi et al. (1998)
CYP79B2	At4g39950	Tryptophan N-monooxygenase 1	Converts Trp to IAOx, precursor to IAA and indole glucosinolate biosynthesis	Bak et al. (1998)
CYP83A1	At4g13770	(methylthio) alkanaldoxime N-monooxygenase	Initial conversion of aldoximes to thiohydroximates in aliphatic glucosinolate biosynthesis	Bak and Feyereisen (2001)
MYB51	At1g18570	Member of the R2R3-MYB transcription family	Promotes Indole glucosinolate biosynthesis	Kranz et al. (1998)
MYB34	At5g60890	Myb-like transcription factor	Modulates expression of ASA1, a key point of control in indole glucosinolate pathway	Bender and Fink (1998)
MYB29	At5g07690	Transcription factor MYB	Promotes aliphatic glucosinolate biosynthesis	Kranz et al. (1998)
PAL1	At2g37040	Phenylalanine ammonia-lyase activity	Biosynthesis of products based on the phenylpropane skeleton from L-phenylalanine	Wanner et al. (1995)
CHS	At5g13930	Chalcone and stilbene synthase family protein	Biosynthesis of flavonoids, accumulation of purple anthocyanins, regulation of auxin transport	Feinbaum and Ausubel (1992)
CHI	At3g55120	Chalcone-flavanone isomerase family protein	Conversion of chalcones into flavanones, accumulation of purple anthocyanins	Kubasek et al. (1992)
MYB4	At4g38620	Member of the R2R3-MYB transcription family	Repressor of target gene expression, one of them encodes cinnamate 4-hydroxylase (flavonoid)	Kranz et al. (1998)
MYB75	At1g56650	Putative MYB domain containing transcription factor	Promotes phenylpropanoid biosynthesis	Kranz et al. (1998)
MYB12	At2g47460	Member of the R2R3-MYB transcription family	Promotes phenylpropanoid biosynthesis	Kranz et al. (1998)

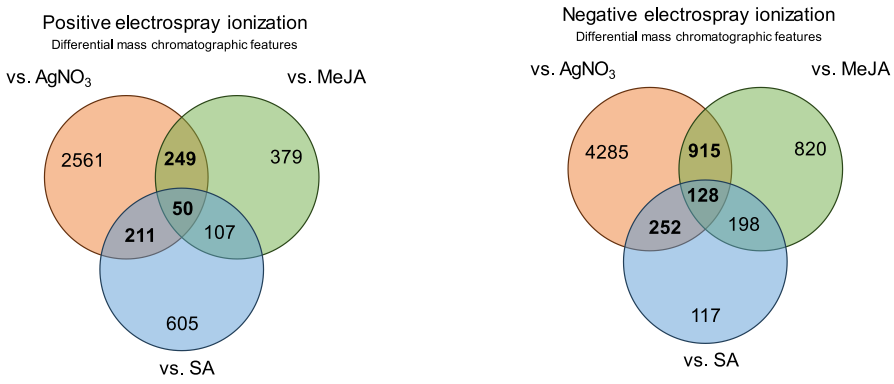

Fig. 1. Venn diagrams depicting the number of differential mass chromatographic features (increased or decreased) in response to $AgNO_3$, MeJA or SA elicitation in *Arabidopsis thaliana*. Values in bold are mass chromatographic features potentially altered by $AgNO_3$ and MeJA or SA.

2.5. Total RNA extraction, purification, and cDNA synthesis

Extraction of total RNA was achieved with the RNeasy mini kit (Qiagen, Valencia, CA, USA), following the manufacturer's instructions with some slight modifications. Briefly, c.a. 50 mg of powdered frozen plant tissue was extracted at 56 °C in the extraction buffer supplemented with β-mercaptoethanol and centrifuged to remove debris. The clean extract was then passed through the kit column, that was washed and eluted according to the manufacturer's instructions. RNA quality and concentration was assessed spectrophotometrically with a Nanodrop (ThermoFisher, USA) and 2 μg of total RNA, that was previously incubated with DNAse to remove genomic DNA, was employed for the cDNA synthesis using the PrimeScript™ RT kit (TaKaRa Bio Europe, France).

2.6. Specific primer design and RT-qPCR analyses

RT-qPCR primers design of the genes of interest (Table 2) was attained using coding sequences of genes (Supplementary Table 2) retrieved from TAIR (www.arabidopsis.org) and the PrimerQuest™ Tool at the IDT website (https://eu.idtdna.com/pages/tools/primerquest?returnurl=%2FPrimerquest%2FHome%2FIndex) setting up the following conditions: amount of GC between 50 and 65%, optimal primer Tm of 62 °C and amplicon size between 100 and 150 nt, also ensuring that primer sequences did not enable the formation of hairpins or primer dimers.

Gene expression by RT-qPCR was performed with the specific gene forward and reverse primer pairs, dNTPs, and SYBR green Master Mix (Thermo Fisher, USA). Reactions were performed in a RT-qPCR thermal cycler (StepOne plus, Applied Biosystems, USA) with the following conditions set up: initial step of 10 min at 95 °C, and then 40 cycles consisting of 10 s at 95 °C followed by 10 s at 60 °C and 20 s at 72 °C. At the end of each run, a melting step (a 0.5 °C s^{-1} ramp from 60 °C to 95 °C) was included to test the specificity of the gene amplification. Relative gene expression values were calculated using the actin gene as internal reference (AT5G09810) following the $2^{-\Delta\Delta Ct}$ method and the REST™ software (Pfaffl, 2002). Each gene was analyzed by triplicate (n = 3, biological replicates) and each sample was analyzed in duplicate (n = 2, technical replicates).

3. Results & discussion

In recent years, inorganic materials at the nano scale or nanomaterials have drawn interest as elicitors of plant defenses in agriculture at non-pollutant concentrations (González-García et al., 2023). Particularly, silver nanoparticles have been shown to trigger specialized metabolite production in different plant species (Cessur et al., 2023; Liu et al., 2022) and ameliorate the damaging effects of abiotic (Khan et al., 2020) and biotic stresses (Kruszka et al., 2020). However, the specific mechanism by which silver materials elicit these responses still remains unknown, although a potential role of JA and SA signaling has long been hypothesized. Therefore, to unravel the involvement of JA and SA in the $AgNO_3$-dependent elicitation of specialized metabolite accumulation, several experiments using *Arabidopsis thaliana* mutants deficient in JA or SA signaling and in key genes involved in specialized metabolite biosynthesis were carried out.

3.1. Identification of specialized metabolite profiles altered by exogenous $AgNO_3$, MeJA and SA treatments

In a first set of experiments, the specialized metabolite profiles of Col-0 plants harvested 24 h after spraying with each of the elicitor molecules were analyzed. The analysis was carried out using reversed phase liquid chromatography which allows a proper separation of compounds ranging from semi-polar to relatively non-polar, hence covering mostly specialized metabolites (Allwood et al., 2008). As a proxy to the ability of each treatment to elicit specialized metabolites, the differentially accumulated mass chromatographic features (mz_Rt values) were used and compared using a mz and Rt matching algorithm. This approach enabled the investigation of the number of overlapping significantly altered mass chromatographic features (with identical mz and Rt values) among treatments (Fig. 1). As a result of the elicitation, the highest impact on the alteration of Col-0 specialized metabolite concentrations was achieved after spraying plants with $AgNO_3$, with 3071 and 5580 differential mass chromatographic features in positive and negative electrospray profiles, respectively. Treatments with MeJA rendered 785 and 2061 whereas SA produced 973 and 695 differentially accumulated features, respectively. These results confirmed the high effectiveness of $AgNO_3$ as elicitor of the specialized metabolism. Few features were shared by the three elicitor treatments, only 50 and 128 (positive and negative ionization), 1.2% and 2.0% of all differential features, respectively. This suggested that the joint contribution of both regulators to the differential accumulation of specialized metabolites is very low. The highest degree of overlapping was found between the $AgNO_3$ and MeJA treatments with 249 and 915 shared features (positive and negative ionization), a 3.75% and 16.4%, respectively. Nevertheless, there were a sheer number of mass chromatographic features obtained after $AgNO_3$ elicitation that did not overlap with those altered by MeJA or SA treatments, that were regarded as a specific response to $AgNO_3$ (Fig. 1).

To investigate the role of JA or SA signaling (or both) in the regulation of the differential accumulation of specialized metabolites in *Arabidopsis thaliana*, Col-0 and deficient in SA or JA signaling plants, *npr1-2* and *coi1-16* mutants, were subjected to MeJA, SA or $AgNO_3$ treatments. Leaf rosettes were sampled 24 h after treatments and

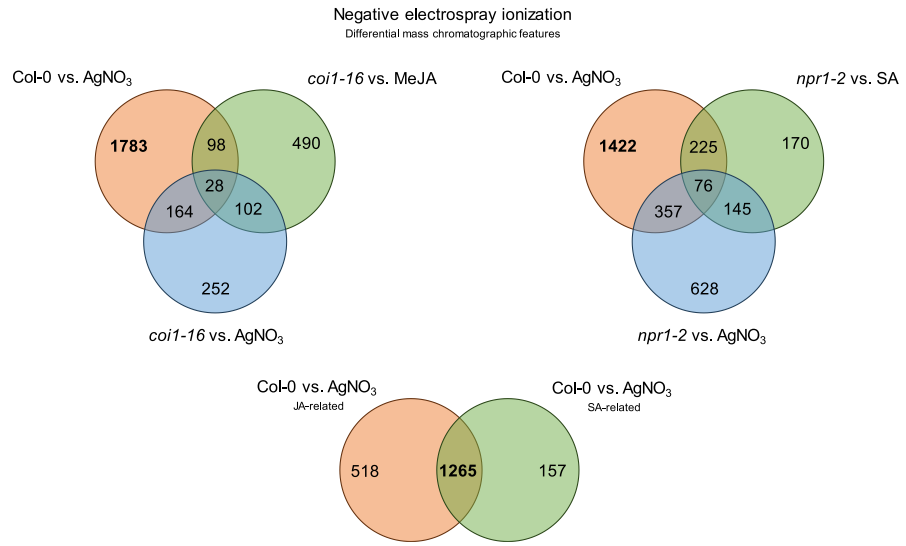

Fig. 2. Venn diagrams depicting the number of differential mass chromatographic features (increased or decreased) in response to $AgNO_3$, MeJA or SA elicitation in Col-0 and *coi1-16* or *npr1-2 Arabidopsis thaliana* mutants. Values in bold are mass chromatographic features potentially altered by $AgNO_3$ and MeJA or SA.

metabolite profiles analyzed as above, followed by a differential mass chromatographic feature overlapping test. The highest impact of the treatments on the specialized metabolism was particularly evident in the negative ionization mode, therefore only this one is presented in Fig. 2, although this test was performed on both ionization modes with similar results (Supplementary Fig. 1).

In this study, those differential mass chromatographic features not overlapping with any of the treatments were the ones of the utmost importance since they could not be linked to SA or JA signaling. There were several differential mass chromatographic features that overlapped among the three groups (28 and 76, JA- and SA-dependent, respectively) that were attributed to a general response to an exogenous chemical treatment. Higher number of differential mass features were found between two individual treatments: 98 and 164 between $AgNO_3$ in Col-0 and MeJA or $AgNO_3$ in *coi1-16*, respectively; whereas 225 and 357 differential mass chromatographic values were found in common with *npr1-2* plants treated with SA or $AgNO_3$, respectively. In all cases (Figs. 1 and 2), $AgNO_3$ alone had a stronger effect on Arabidopsis specialized metabolism than SA or MeJA treatments. The differential mass chromatographic features in $AgNO_3$-treated plants of Col-0 that did not overlap with any of those found in hormone or $AgNO_3$-treated *coi1-16* or *npr1-2* plants (1783 and 1422, respectively) were subsequently subjected to an overlapping test and 1265 (a 65.2%) were common between the two groups (Fig. 2), supporting the notion that these mass chromatographic features were altered by $AgNO_3$-treated putatively through JA and SA signaling. To further investigate this aspect, the common altered mass chromatographic features were identified and annotated (Supplementary Table 1) and represented as heatmap to provide a wide overview of the changes induced by treatments and or genotype (Fig. 3).

3.2. Alteration in specialized metabolite profiles in npr1-2 and coi1-16 arabidopsis mutants

The most prominent effect was observed for all genotypes after treatment with $AgNO_3$ with a clear induction of oxylipins and jasmonates (13(S)-HOTrE, 12-OPDA and JA) and salicylates (SA and SAGE), and defensive compounds such as camalexin and its precursor dihydroxycamalexic acid (DHCA), c- and t-coumaroylagmatins, and 4-MeO-I3M glucosinolate (neoglucobrassicin), showing in general a stronger induction in Col-0 than in *coi1-16* or *npr1-2* (Fig. 3). The phenomenon of specialized metabolite, and particularly phytoalexin, induction by $AgNO_3$ has already been known for decades (Yoshikawa, 1978), but the specific mechanism leading to the metabolic output is, to the best of our knowledge, unknown. Indeed, (Schuhegger et al., 2006) identified, and was further refined by (Böttcher et al., 2009), the multifunctional enzyme CYP71B15, also known as PAD3, as the final step in the biosynthesis of the phytoalexin camalexin, using Arabidopsis mutants, feeding experiments and $AgNO_3$ elicitation as the main experimental tools.

Next, a more in-depth analysis was performed by a 2-way ANOVA on annotated metabolites and only 4 metabolites were significantly altered in the Genotype × Treatment interaction: c-coumaroylagmatin, DHCA, 12-OPDA and camalexin, potentially indicating that these metabolites were not necessarily subjected to the regulation posed by jasmonates or salicylates (Supplementary Table 3). Interestingly, nearly all metabolites annotated showed significant differences associated to Genotype, among which several of them did not show significant differences considering the Treatment factor. These metabolites were essentially AGs and IGs which, in the heatmap, showed clear differences at the basal levels (Fig. 3). This raised the question whether basal metabolite levels could influence the final metabolite output upon $AgNO_3$ or hormone elicitation and, more importantly, whether they could influence overall hormonal signaling. To investigate this aspect, a new set of experiments including Arabidopsis genotypes with different accumulation of specialized metabolites was carried out, focusing on glucosinolates as this metabolite class was the most prominent in the list of annotated differential metabolites (Supplementary Table 1).

3.3. Alterations in the indole compound pool are associated to JA and SA hormonal signaling

Plants of the indole glucosinolate overaccumulator *atr1D*, the IG deficient *cyp79b2/cyp79b3* and the IG and AG deficient *myb28/myb29/cyp79b2/cyp79b3* (qKO) (Table 1) were grown and assayed as previously indicated. As expected, indolic compound levels in *atr1D* were higher than in Col-0 (Fig. 4 and Supplementary Table 4) with an apparent side-effect on quercetin derived flavonoids and phenylpropanoids (scopolin sinapic acid derivatives, and p-coumaric acid). Interestingly, as hypothesized, the higher accumulation of indolics found in *atr1D* influenced the ability of $AgNO_3$, MeJA and SA to elicit camalexin accumulation, which was significantly lower, and it even reduced the $AgNO_3$-associated accumulation of SA, SAGE, Phe, DHCA, 13(S)-HOTrE, JA-Ile, 12-OPDA and JA. Similarly, metabolite profiles of double mutant *cyp79b2/cyp79b3* devoid in any indolic compound derived from Trp

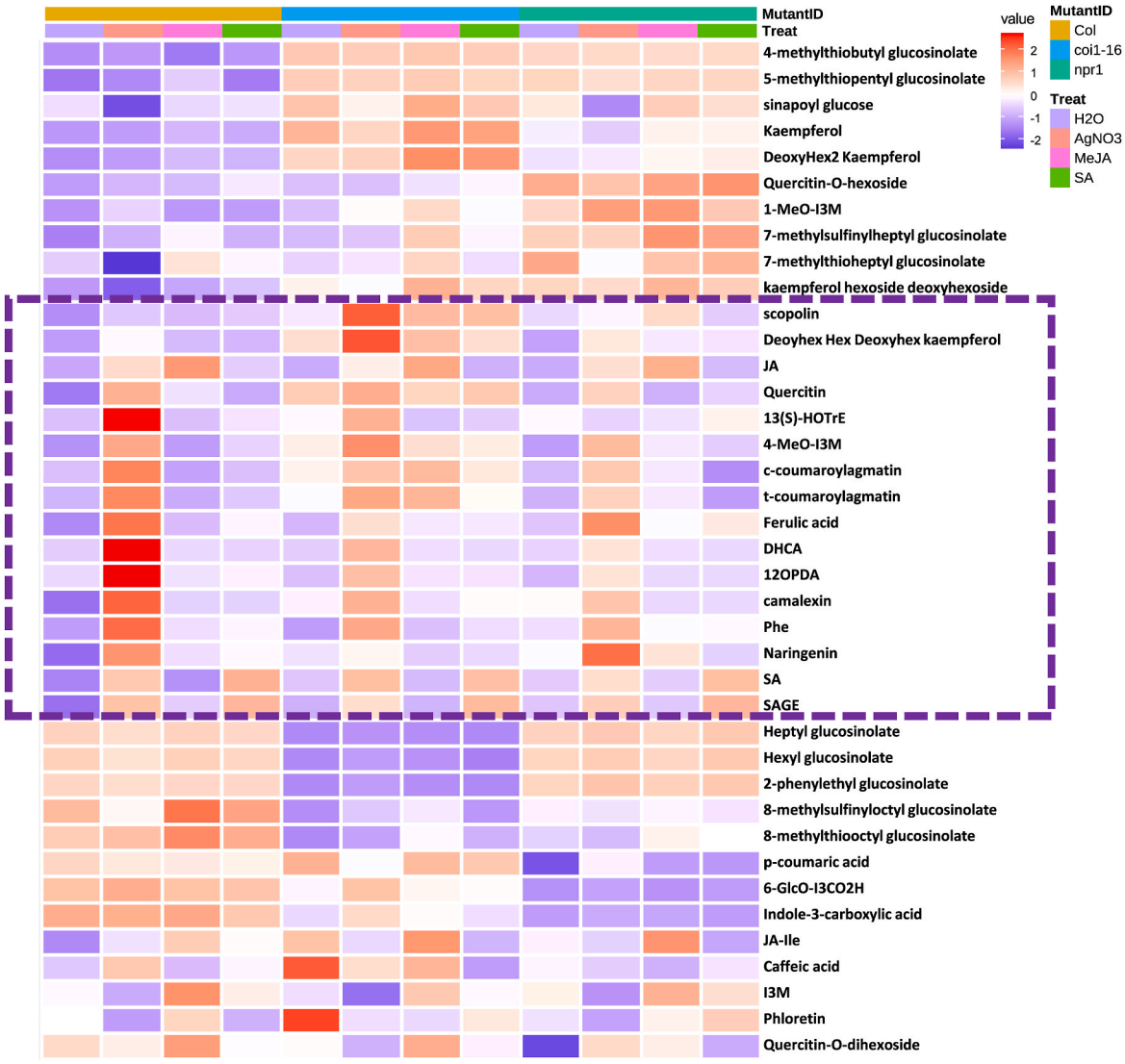

Fig. 3. Changes in levels of glucosinolates, oxylipins, phenolic compounds and flavonoids in mutants affected in JA (*coi1-16*) and SA (*npr1-2*) signaling, compared to Col-0 wild type plants in response to elicitors ($AgNO_3$, MeJA and SA) or mock treatment (water). The purple rectangle highlights metabolites that are specifically induced by $AgNO_3$.

(including indole glucosinolates and the phytoalexin camalexin), also exhibited a reduction in the ability to induce jasmonates, although to a lesser extent than *atr1D*. This mutant also exhibited an impact of the lack of indolics on aliphatic glucosinolate contents (4-methylthiooctyl, 6-methylthiohexyl and heptyl glucosinolates), flavonoids with kaempferol core moiety and c- and t-coumaroylagmatins (Fig. 4). Finally, qKO, which lacks any type of glucosinolate, still retained the ability to induce the same metabolites as Col-0 in response to $AgNO_3$ except for the indolics camalexin and its precursor DHCA, with a clear impact on 13 (S)-HOTrE. Moreover, at the genotype level, the impact on other metabolite classes was higher, including kaempferol derived flavonoids, phenylpropanoids (sinapic acid derivatives, p-coumaric acid and caffeic acid) and c- and t-coumaroylagmatins (Fig. 4).

To test the role of AGs alone, an assay with the *myb28/myb29* mutant challenged with $AgNO_3$ was performed. No differences in the levels of the metabolites altered (signaling jasmonates and defensive compounds camalexin and c-coumaroylagmatin) respect to Col-0 were observed except for a reduction in the maximum build-up of SA and SAGE (Supplementary Fig. 2). Overall, the results indicate that, at the metabolic level, there is a clear interplay between IGs (but not AGs) and the signaling molecules SA and JAs, and that the ability to respond to exogenous elicitor molecules, such as $AgNO_3$ is modulated by the basal IG levels.

3.4. Defective JA and SA signaling impacts on IGs metabolism

To characterize the metabolic response at the molecular level, the expression of different biosynthetic and regulatory genes in Arabidopsis was analyzed under the conditions assayed (Table 2). As a general trend, $AgNO_3$ induced the expression of MYB51, a TF involved in indole glucosinolate biosynthesis, but it was much lower in *npr1-2* and *coi1-16* mutants than in Col-0. Paralleling MYB51 induction, treatment with $AgNO_3$ repressed MYB29 expression, involved in AG biosynthesis (Fig. 5). On the contrary, both MeJA and SA treatments repressed MYB51 expression. The expression trend of MYB51 correlated with that of CYP79B2 (Fig. 5) in line with their regulatory association (Frerigmann et al., 2016). These results are in accordance with the induction of CYP79B2 by MeJA in the *npr1-2* mutant which was higher than in the *coi1-16* mutant. On the other hand, SA application barely changed basal CYP79B2 expression, except for npr1-2 in which it showed negative $\log_2$ fc values. These results suggest that $AgNO_3$-dependent CYP79B2 induction through MYB51 regulation is partially dependent on JA and SA

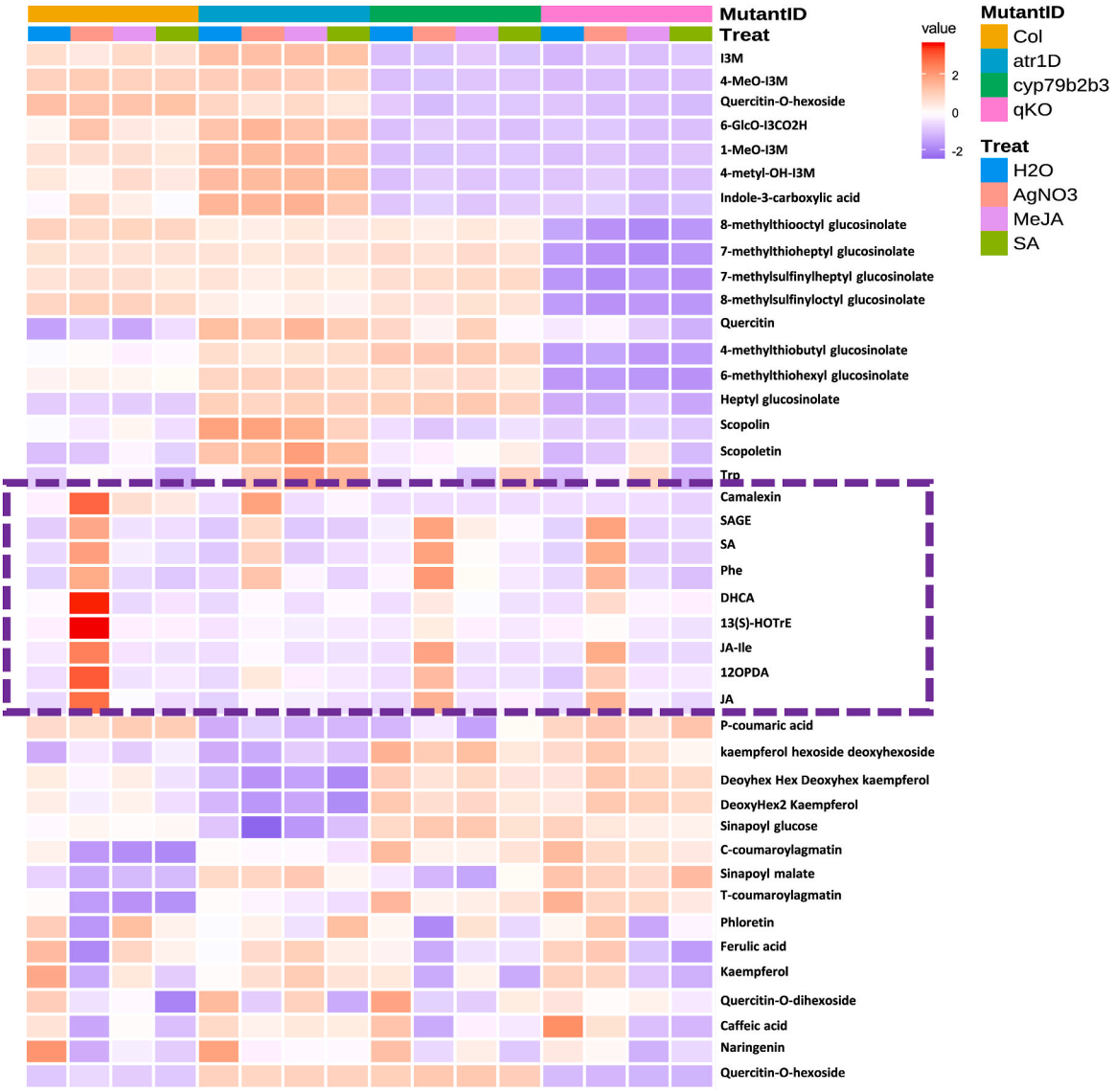

Fig. 4. Changes in levels of glucosinolates, oxylipins, phenolic compounds and flavonoids in indole glucosinolate overaccumulators (*atr1D*, MYB34-OE), indole glucosinolate devoid (*cyp79b2/cyp79b3*) and glucosinolate devoid (qKO, *myb28/myb29*), compared to Col-0 wild type plants in response to elicitors ($AgNO_3$, MeJA and SA) or mock treatment (water). The purple rectangle highlights metabolites that are specifically induced by $AgNO_3$.

signaling, although certain uncoupling between MYB51 and CYP79B2 expression might exist, potentially involving other TFs such as MYB34/ATR1. Interestingly, MYB34/ATR1 expression was highly induced upon $AgNO_3$ treatment in *npr1-2* seedlings suggesting a potential crosstalk between MYB51 and MYB34 to promote indole compound biosynthesis, possibly through JA signaling (Frerigmann et al., 2021; Frerigmann and Gigolashvili, 2014). Therefore, given the reported antagonism between SA and JA signaling pathways (Leon-Reyes et al., 2010; Van der Does et al., 2013), it seems logical that JA signaling driving MYB34 expression is enhanced in *npr1-2* mutants. In addition, this response was not observed in *coi1-16* seedlings after $AgNO_3$ nor in Col-0 after $AgNO_3$, MeJA or SA spraying (Fig. 5A). The expression of MYB29 TF, involved in AG biosynthesis, was downregulated by $AgNO_3$, and it was clearly correlated with CYP83A1 expression, the first committed step in AG biosynthesis (Fig. 5A). This response was not abolished in *npr1-2* or *coi1-16* mutants and even the downregulation observed in Col-0 was exacerbated. Strikingly, no clear induction of CYP83A1 could be observed in response to MeJA or SA except for *npr1-2* in which its expression was induced by MeJA (Fig. 5). This response is also correlated with the reduced basal levels of certain AGs in *coi1-16* that were enhanced in *npr1-2* respect to Col-0 (Fig. 3).

The MYB4 TF has been reported to act as a repressor of sinapate ester biosynthesis in *Arabidopsis thaliana* (Liu et al., 2015 and references therein) whereas MYB12 and MYB75 act as activators of biosynthesis of flavonol/chlorogenic acid and most phenylpropanoids. We have found that MYB4 gene expression is reduced in Col-0 and *coi1-16* in response to all treatments. However, in *npr1-2* the outcome was completely opposite to that of *coi1-16* showing a clear upregulation, being highest upon MeJA and SA treatments (Fig. 5B). This upregulation of the repressor MYB4 TF in *npr1-2* mutant was correlated with a general downregulation of MYB75 in this genotype, which was upregulated in Col-0 by MeJA and, to a lower extent, by $AgNO_3$. On the contrary, SA treatment did not have any significant effect on the expression of MYB75 in Col-0 and *coi1-16*, showing even a slight downregulation. However, in *npr1-2*, $AgNO_3$ and SA did induce a stronger downregulation of MYB75 suggesting the active participation of SA signaling. The expression of the activator TF MYB12, involved in flavonol and chlorogenic acid biosynthesis induction, was repressed in response to all elicitor treatments in Col-0, whereas $AgNO_3$ and MeJA treatments repressed the expression of this gene in the *npr1-2* mutant and only $AgNO_3$ had the same effect in

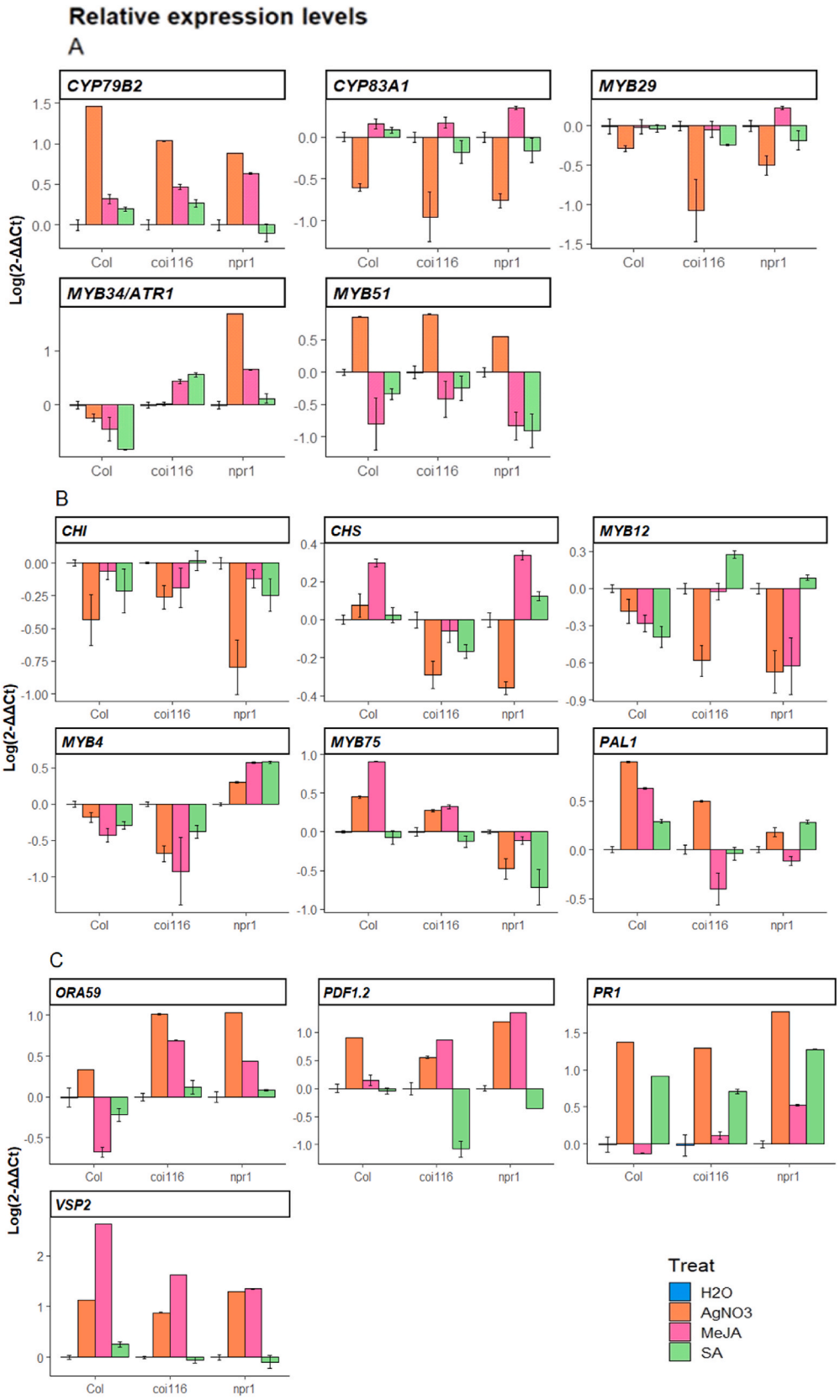

Fig. 5. Changes in the expression profile of genes involved in indole and aliphatic glucosinolate biosynthesis: A) CYP79B2, CYP83A1, MYB34, MYB29 and MYB51, genes involved in phenylpropanoid and flavonoid biosynthesis: B) CHI, CHS, PAL1, MYB12, MYB4 and MYB75, and genes involved in JA and SA signaling. C) ERF1 branch: OR59 and PDF1.2 and MYC2 branch: VSP2, and PR1.

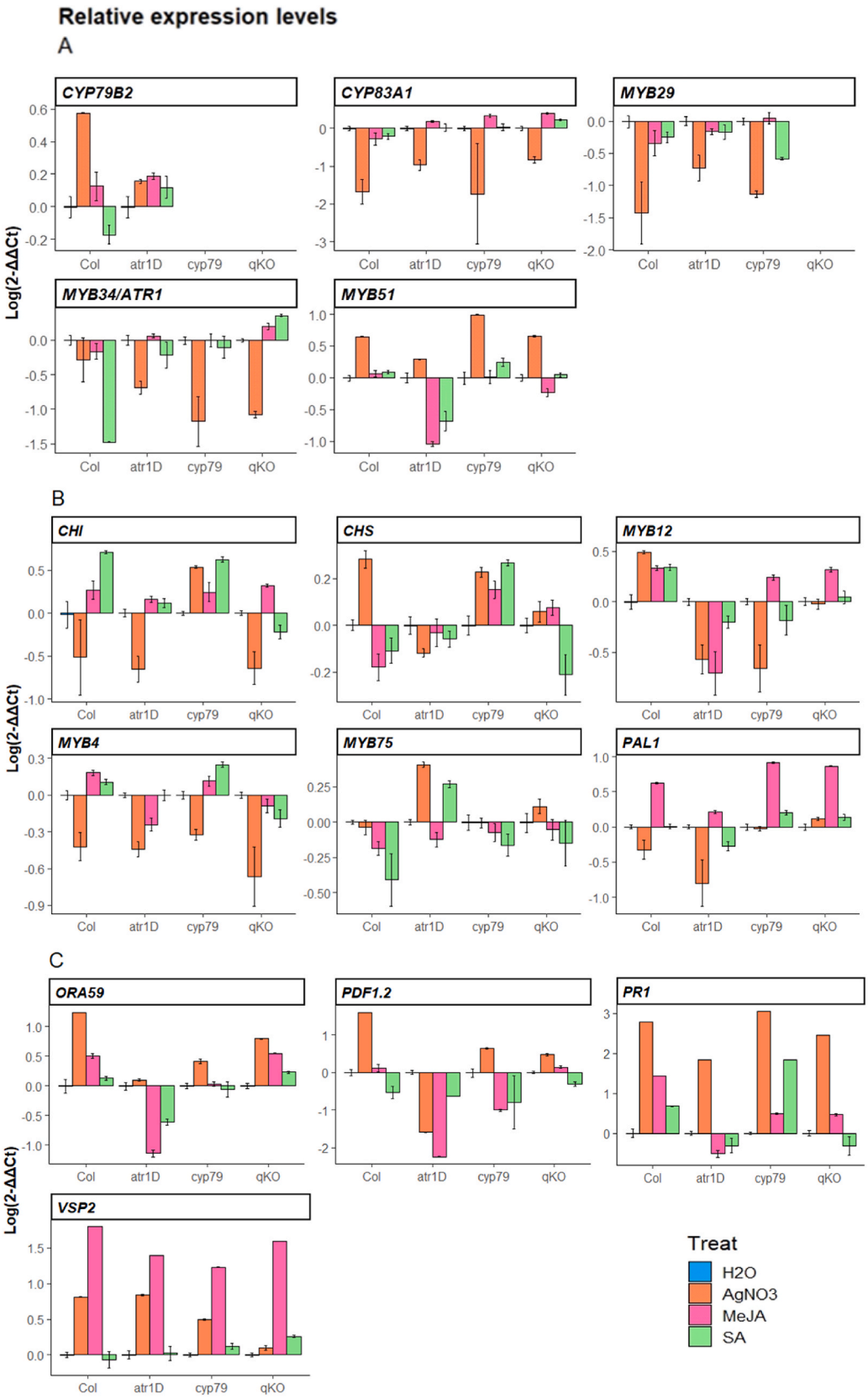

Fig. 6. Changes in the expression profile of genes involved in indole and aliphatic glucosinolate biosynthesis: A) CYP79B2, CYP83A1, MYB34, MYB29 and MYB51, genes involved in phenylpropanoid and flavonoid biosynthesis: B) CHI, CHS, PAL1, MYB12, MYB4 and MYB75, and genes involved in JA and SA signaling. C) ERF1 branch: OR59 and PDF1.2 and MYC2 branch: VSP2, and PR1.

coi1-16. Conversely, in these genotypes, SA treatment induced the overexpression of MYB12, much lower in *npr1-2* (Fig. 5B). Following MYB75 expression, the PAL1 gene expression was clearly and significantly upregulated in Col-0 in response to all treatments, exhibiting the highest upregulation upon $AgNO_3$ spraying, followed by MeJA and then SA. Much lower was the expression of PAL1 found in *coi1-16* which was highest in seedlings treated with $AgNO_3$, with no significant difference upon SA treatment and with a significant repression in seedlings treated with MeJA. In turn, CHS (the first key committed step in flavonoid biosynthesis) responded primarily to MeJA treatment in all seedlings except in the *coi1-16* seedlings (Fig. 5B) whereas in this and in *npr1-2* seedlings, $AgNO_3$ caused a repression of CHS expression. A similar response was observed for CHI (the second step in flavonoid biosynthesis following CHS), but without a clear upregulation observed in MeJA-treated seedlings. These results indicate that phenylpropanoid biosynthesis depends on SA signaling more than on JA signaling whereas flavonoid biosynthesis seems to be exclusively dependent on JA signaling. On the signaling aspect, $AgNO_3$ seems to activate both SA (PR1) and the ERF1 branch (PDF1-2 and ORA59) of JA signaling whereas the MYC2 branch (VSP2) of JA signaling seems to be less responsive to $AgNO_3$ treatment. Interestingly, both ERF1 and MYC2 branches were unresponsive to SA treatment and the PR1 gene did not respond to MeJA treatment, supporting the notion that $AgNO_3$ treatment exerts its effect on specialized metabolism partially through SA and the JA pathways and, more precisely, through the JA/ERF1 branch (Fig. 5C). These results are in line with those published by (Kliebenstein et al., 2002) which indicated a complex regulation of IGs production by MeJA involving at least three pathways and a crosstalk with SA

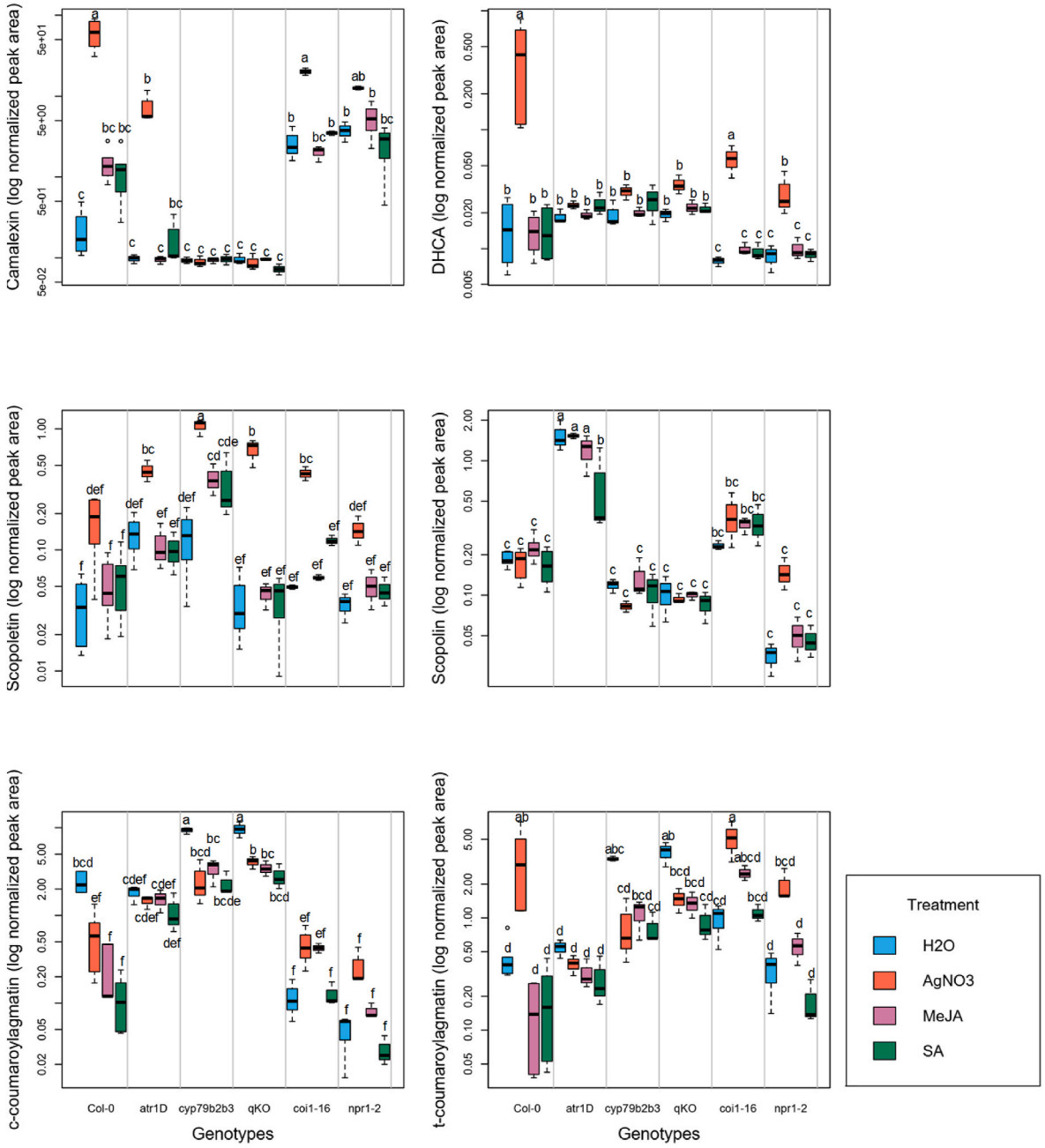

Fig. 7. Log-normalized peak area values of selected metabolites (camalexin, dihydrocamalexic acid or DHCA, scopoletin, scopolin, c- and t-coumaroylagmatins) involved in plant defense, regulated by $AgNO_3$ and SA or MeJA. Boxes with different letters denote statistically significant differences at $p \leq 0.05$ after 2-way ANOVA and Tukey posthoc test.

signaling.

3.5. Overaccumulation of IGs downregulates JA and SA signaling

The gene expression of biosynthetic and regulatory genes in Arabidopsis mutants with altered endogenous levels of glucosinolates was also analyzed. As observed in the previous experiment, $AgNO_3$ treatment induced expression of MYB51 but repressed MYB34 and MYB29 in all Arabidopsis genotypes (Fig. 6A). In addition, as expected, no MYB29 or CYP79B2 expression could be detected in qKO mutants. Interestingly, MYB51 expression was highest in *cyp79b2/cyp79b3* mutants followed by Col-0 and qKO and much lower in *atr1D* seedlings. Likewise, CYP79B2 expression was induced by $AgNO_3$ in Col-0 but not in *atr1D* seedlings, despite IGs levels were significantly much higher in this genotype (Fig. 4 and Supplementary Table 4). As already reported in (Celenza et al., 2005), *atr1D* seedlings do not display a particularly enhanced expression of MYB34 but exhibit an impact on CYP79B2 and CYP79B3 expression. In this work, $AgNO_3$, MeJA or SA treatments had a marginal effect on CYP79B2 expression in *atr1D,* suggesting the retrograde involvement of IGs on the $AgNO_3$-dependent induction of this gene. As in the previous set of experiments, expression of MYB29 and CYP83A1 was severely repressed by $AgNO_3$ in all genotypes. As already observed, CYP83A1 expression was induced by MeJA to a higher extent in qKO and *cyp79b2/cyp79b3* and only slightly in *atr1D* seedlings, but not in Col-0 (Fig. 6A). Overall, these data suggest that regulation of indole compound biosynthesis is primarily induced by $AgNO_3$ through MYB51 expression and high basal IG levels exert a negative feedback regulation on its expression. Moreover, $AgNO_3$ treatment had a negative impact on CYP83A1 expression but without any significant effect on metabolite accumulation (Figs. 4 and 6A).

In this set of experiments, expression of MYB75 gene, the main responsible for phenylpropanoid and flavonoid biosynthesis, remained near to control levels in all genotypes except in the *atr1D* mutant in which $AgNO_3$ and SA treatments induced its expression; however, this was not correlated with a parallel overexpression of CHS, CHI or PAL1 genes (Fig. 6B). The other activator TF, MYB12, responded positively to all three treatments in Col-0 whereas in the *atr1D* it was repressed in response to all treatments. Furthermore, in the *cyp79b2/cyp79b3* background, $AgNO_3$ treatment reduced MYB12 expression, whereas MeJA increased it (Fig. 6B). A similar trend was observed in qKO seedlings, except that $AgNO_3$ treatment did not repress MYB12 gene expression. In turn, MYB4 gene expression was consistently repressed by $AgNO_3$ treatment in all genotypes and induced by MeJA and SA treatments in Col-0 and *cyp79b2/cyp79b3* mutant, whereas it was repressed by MeJA in *atr1D*. Taken together, these results indicate that flavonoid regulation is indeed very complex and the interaction of the activators MYB75 and MYB12 with repressor MYB4 could render multiple outcomes. Recently, (Naik et al., 2023) showed a crosstalk between flavonols and indole compounds in the absence of any challenging treatment. In their work, Arabidopsis *fls1* mutants, devoid in the flavonols quercetin and kaempferol, showed enhanced basal camalexin levels, albeit a reduction in indole glucosinolate levels, coincident with an upregulation of CYP79B2, CYP79B3 and PAD3 genes whereas genes involved in AGs biosynthesis (MYB29, CYP83A1, CYP79F1 and CYP79F2) were repressed respect to wild type. This points out a channeling of indole compound metabolism to the synthesis of the phytoalexin camalexin in the absence of the other protective compounds, flavonoids. In this work, *atr1D* exhibited enhanced basal levels of scopolin and scopoletin, sinapoyl malate ferulic and caffeic acids and quercetin-derived flavonoids (Fig. 4). A similar pattern was observed in *cyp79b2/cyp79b3*, with the accumulation of kaempferol derivatives, sinapoyl glucose and c- and t-coumaroylagmatins instead of scopolin and scopoletin upregulation. Interestingly, in qKO elevated sinapoyl malate and p-coumaric acid besides the metabolic shift observed in *cyp79b2/cyp79b3*. Interestingly, these results indicate that alterations in IG levels are the driving force in the observed metabolic shifts.

Focusing on the signaling events, $AgNO_3$ treatments elicited the activation of both SA and JA signaling pathways, as already observed in the first set of experiments. The upregulation of indole compound biosynthesis in the *atr1D* mutant severely reduced the output of both SA and JA pathways (reduced the expression of PR1, PDF1.2, and ORA59 genes). In *cyp79b2/cyp79b3* mutant, JA signaling (PDF1.2, VSP2 and ORA59) was reduced but not abolished, whereas SA signaling (PR1) was enhanced. These results indicate a clear crosstalk between indole glucosinolate accumulation and JA and SA signaling. Knocking down both AGs and IGs biosynthesis did not modify the pattern of the JA signaling response respect to Col-0, but reduced the output level, and for the JA/MYC2 branch, reduced the responsiveness to $AgNO_3$ (Fig. 6C). However, the SA signaling pathway was less affected, as evidenced by the strong upregulation of PR1 gene in *cyp79b2/cyp79b3* or qKO mutants after $AgNO_3$. As in the former set of experiments, the expression of VSP2 (MYC2 branch) responded primarily to MeJA treatment and, more moderately, to $AgNO_3$. Moreover, VSP2 gene expression levels were clearly reduced in *atr1D* and *cyp79b2/cyp79b3* backgrounds in response to MeJA. In qKO, VSP2 expression in response to $AgNO_3$ was completely abolished but response to SA was partially restored, reinforcing the notion of a complex crosstalk between glucosinolates and signaling pathways. The expression of ORA59 and PDF1.2 genes was induced by $AgNO_3$ in Col-0, to a much lesser extent in *cyp79b2/cyp79b3* and qKO mutants and completely abolished or even repressed in *atr1D*. This indicates that alteration in indole compound abundance, as in *atr1D*, *cyp79b2/cyp79b3* or qKO mutants, affects JA signaling both a the signaling compound accumulation and at the molecular level (Figs. 4 and 6C).

3.6. Accumulation of defense compounds in arabidopsis is driven by hormonal and metabolic signals

The levels of known defensive compounds in *Arabidopsis thaliana* was explored in detail in the different genotypes studied and shown in Fig. 7. Results were expressed as log-transformed normalized peak area values to facilitate representation, but calculations on fold changes were performed on normalized peak area values (to ISTD area and sample fresh weight). The levels of the phytoalexin camalexin and its precursor dihydrocamalexic acid (DHCA) were also explored. Levels of DHCA were not significantly different among treatments in *atr1D*, *cyp79b2/cyp79b3* and qKO mutants, whereas higher levels were found in Col-0 and to a lower extent in *coi1-16* and *npr1-2* mutants in response to $AgNO_3$, which partially correlated with the accumulation of camalexin. Significant levels of camalexin were found in all genotypes except *cyp79b2/cyp79b3* and qKO mutants, as expected. The highest levels of camalexin were observed in Col-0, followed by *coi1-16* and *npr1-2* mutants, in response to $AgNO_3$ treatment. Only Col-0 responded to MeJA and SA treatments and showed a significant accumulation of camalexin. Interestingly, the *atr1D* mutant, which can accumulate higher amounts of indolic compounds, did not show such huge amounts of camalexin. This could be associated to a different channeling of indolics or perhaps to the existence of a downstream regulatory point specific of the camalexin pathway (Celenza et al., 2005), although a specific effect on JA and SA signaling pathways cannot be ruled out. To this respect, the high amounts of camalexin found in *npr1-2* and *coi1-16* mutants despite not as high as in Col-0, point towards the partial participation of both JA and SA signaling pathways.

The coumarin glycoside scopolin showed identical levels in all genotypes except in *coi1-16* and *atr1D* mutants in which levels were 1.6 and 6 times higher, respectively. However, no specific pattern of induction in response to each of the exogenous treatments could be observed; except for the *atr1D* mutant in which SA caused a significant reduction of these metabolites respect of basal levels. In the *npr1-2* mutant, scopolin levels were lower than in Col-0 but, conversely, responded to $AgNO_3$ elicitation. Interestingly, the aglycon scopoletin did generally respond to $AgNO_3$ and, in some genotypes, also to MeJA and

SA treatments. Highest levels were found in *cyp79b2/cyp79b3*, followed by qKO after treatment with $AgNO_3$.The *cyp79b2/cyp79b3* genotype also responded to MeJA and SA treatments rendering significantly increased scopoletin levels whereas in the *coi1-16* background, it responded to SA but not to MeJA treatment (Fig. 7).

Finally, the levels of c- and t-coumaroylagmatins were investigated. Levels of c-coumaroylagmatin responded negatively to all exogenous treatments except in *coi1-16* and *npr1-2* mutants. In fact, the application of $AgNO_3$, MeJA or SA treatments reduced endogenous c-coumaroylagmatin levels in Col-0, *cyp79b2/cyp79b3* and qKO genotypes, being the strongest effect that exerted by SA treatment (Fig. 7). In the *atr1D* mutant, this effect was more moderate and only seedlings treated with SA displayed a significant reduction in c-coumaroylagmatin. Basal levels of c-coumaroylagmatin were higher in *cyp79b2/cyp79b3* and qKO mutants, and much lower (~96% reduction respect to Col-0) in *npr1-2* and *coi1-16* mutants. These two genotypes also differed from the rest in the fact that they responded positively to $AgNO_3$ treatment, showing significantly different levels of c-coumaroylagmatin. In turn, the accumulation profile of t-coumaroylagmatin almost mirrored that of c-coumaroylagmatin except for Col-0 that did respond to $AgNO_3$ treatment and displayed significantly elevated levels of this metabolite. Again, the *atr1D* mutant did not show any significant variation in the levels of c- or t-coumaroylagmatins in response to exogenous treatments. The mutant lines *cyp79b2/cyp79b3* and qKO showed significantly reduced levels in response to all elicitation treatments, but displayed significantly higher basal levels compared to Col-0 (Fig. 7). Both *coi1-16* and *npr1-2* mutants responded to $AgNO_3$ treatment and displayed elevated t-coumaroylagmatin levels. These results suggest the existence of a metabolic regulatory loop involving actual metabolite levels. When basal levels of coumaroylagmatins or indolic compounds are above a certain threshold, the response to exogenous treatments seems to be reduced or even abolished and, in some cases, a repression of the accumulation of these metabolites respect to basal levels is observed. Conversely, when basal levels are low, plants can respond to elicitor treatments and accumulate significant amounts of these defensive compounds. Similarly, elevated levels of indolic glucosinolates seem to hinder the accumulation of c- or t-coumaroylagmatin and, on the contrary, plants devoid in these compounds show enormous basal amounts of polyamine-phenylpropanoid conjugates.

Taken together, results indicate that the $AgNO_3$ treatment exerts its effects through the activation of JA and SA signaling pathways since mutants *coi1-16* and *npr1-2* displayed a clear impact on their metabolic outcome (Fig. 3) after elicitation and also showed an altered basal metabolite accumulation (particularly depicted by elevated levels of IGs and AGs). Moreover, by using mutants altered in IGs and AGs contents (*atr1D*, *cyp79b2/cyp79b3*, *myb28/myb29*, and qKO), it was found that the overaccumulation of IGs downregulated both SA and JA signaling pathways. Knocking down IGs or IGs and AGs glucosinolate pools had different effects, while the *cyp79b2/cyp79b3* mutant showed a reduced JA signaling, it enhanced SA signaling; nevertheless, knocking down both glucosinolate pools severely reduced the JA/ERF1 pathway (ORA59 and PDF1.2) as well as SA signaling in response to the elicitor treatments (Fig. 6). When only AGs were reduced, only a mild effect on SA accumulation after challenging with $AgNO_3$ was observed. At the metabolic level, *atr1D*, *cyp79b2/cyp79b3* and qKO mutants showed clearly low levels of $AgNO_3$-induced specialized metabolites, including signaling molecules such as salicylates and oxylipins (Fig. 4), suggesting a systemic effect of the metabolic alteration induced by mutations. Likewise, hormone signaling mutants also displayed an altered ability to induce this set of $AgNO_3$-induced metabolites, in some cases linked to altered basal levels of metabolites, which is probably connected to the signaling alteration itself.

To the best of our knowledge, this is the first-time that evidence of a clear crosstalk between specialized metabolites and hormonal signaling pathways is shown, thus supporting the notion that specialized metabolites can also play a signaling role (Gao et al., 2023).

In other plant species of the Brassicaceae family, it has been shown that application of MeJA induces the accumulation of IGs through induction of CYP79s-encoding genes putatively regulated by MYB34 and MYB51 TFs (Wiesner et al., 2013; Zang et al., 2015). Moreover, in *Brassica rapa*, the potential of MeJA to induce IGs was higher than that of SA and both regulators reduced total AGs accumulation (Schreiner et al., 2011). However, it remains unclear how the specific contribution of each hormonal pathway led to the metabolic output. In resistant and susceptible lines of *B. rapa*, challenging plants with the necrotrophic bacterium *Pectobacterium brasiliense* caused the accumulation of JA and JA-related transcripts (JA-dependent transcription repressors JAZ genes) along with IGs 24 h post inoculation. Interestingly, regulatory and biosynthetic genes (*BrMYB51*, *BRST5a*, *BrCYP81F4* and *BrIGMT1*) did not follow the same trend and displayed a maximum expression earlier after the inoculation (Yi et al., 2022). The data presented in this manuscript are consistent with these previous reports and extend the findings to the interplay between regulatory and signaling metabolites as well as the mechanism by which $AgNO_3$ elicits plant specialized metabolites.

4. Conclusions

It has been known for decades that silver nitrate ($AgNO_3$) is a powerful elicitor of the specialized metabolism in several plant species, even at much lower concentrations than other compounds (Yoshikawa, 1978). For this reason, it has been used either as an experimental tool to investigate the specialized metabolism, its regulation and its roles in plant defense against exogenous threats and also as a treatment to prepare crop plants to endure environmental stress (Acharya et al., 2020; Böttcher et al., 2009; Glawischnig et al., 2004).

In this work, $AgNO_3$ treatments have been used to investigate the interaction of the specialized metabolism and defense plant hormone signaling in *Arabidopsis thaliana*. Treatment with 5 mM $AgNO_3$ solution by spraying Arabidopsis leaves had a strong impact on semi-polar compound accumulation only 24 h after treatment, producing an overaccumulation of IGs and camalexin, Phe, phenylpropanoids such as c- and t-coumaroylagmatins and ferulic acid, flavonoids such as kaempferol and quercetin derivatives, along with build-up of jasmonates (12-OPDA and JA), oxylipins (13-HOTrE) and salicylates (SA and SAGE). On JA and SA signaling-deficient Arabidopsis mutants, this accumulation was less pronounced than in Col-0 and even a shift in the basal accumulation of different specialized metabolites was observed (Fig. 3), suggesting that both signaling pathways could be involved, at least partially, in the elicitor role of $AgNO_3$. This was confirmed by gene expression studies which showed a differential upregulation of MYB34, MYB51 and CYP79B2 genes, involved in IGs biosynthesis, in response to $AgNO_3$. Likewise, analysis of marker genes for JA signaling such as PDF1.2 and ORA59 of the ERF1 branch and VSP2 of the MYC2 branch showed an upregulation induced by $AgNO_3$. This upregulation was altered in the JA-defective background, as well as PR1, related to SA signaling (Fig. 5C). When analyzing the metabolomic and transcriptional response of Arabidopsis mutants with increased or decreased production of IGs or AGs, it was found that the overaccumulation of IGs in *atr1D* partially dampened the metabolic response observed in Col-0. Moreover, it shifted the basal metabolite profile showing increased AGs and phenylpropanoids and reduced flavonoids (Fig. 4). Blocking indole compound biosynthesis (*cyp79b2/cyp79b3*) or IGs and AGs (qKO), did not restore Col-0 phenotype in response to $AgNO_3$ but shifted the basal metabolism to an enhanced accumulation of AGs and phenylpropanoids. At the signaling level, $AgNO_3$ treatment in *atr1D* background did not induce PDF1.2 or ORA59 expression, whereas PR1 expression was severely reduced. These genes did not respond either to MeJA or SA treatments in *atr1D*, whereas their response in *cyp79b2/cyp79b3* or qKO was clearly reduced. These results indicate that IGs interact primarily with JA/ERF1 pathway and to a lesser extent with JA/MYC2 pathway, whereas their deficiency causes an upregulation of the

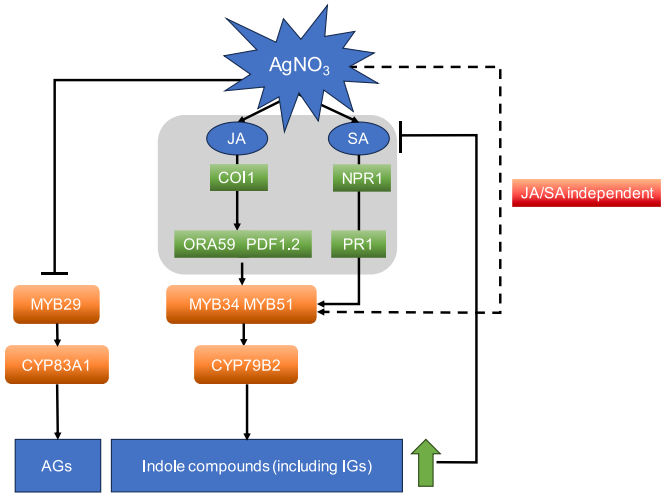

Fig. 8. Proposed model of action of $AgNO_3$ in *Arabidopsis thaliana*.

SA signaling pathway.

Overall, the results presented in this manuscript indicate that, in Arabidopsis, $AgNO_3$ exerts its elicitor activity partially through JA and SA signaling, influenced by the basal amounts of IGs. High basal amounts of IGs strongly dampen JA and SA signaling and reduce the elicitor effect. A model highlighting the results obtained in this work is provided in Fig. 8.

Funding statement

Financial support was provided through projects OPTIMUS PRIME, grant PCI 2021-121920 funded by MCIN/AEI/10.13039/501100011033 and by the "European Union NextGenerationEU/PRTR", EXTREMO grant PID 2020-118126RB-I00 funded by MCIN/AEI/10.13039/501100011033, UJI-B2019-24 and UJI-B2022-23 funded by Universitat Jaume I. Funding from 'Santiago Grisolia' fellowship grant from Conselleria d'Innovació, Universitats, Ciència i Societat Digital (Generalitat Valenciana, CIGRIS/2021/014) to B.O.G. and a predoctoral fellowship from Conselleria d'Educació, Universitats i Ocupació (Generalitat Valenciana, CIACIF/2022/241) to J.M.A. is gratefully acknowledged. M.G-G. particularly acknowledges the support received from the Spanish Ramón y Cajal Program, grant RYC-2016-19325 funded by MCIN/AEI/10.13039/501100011033 and by "ESF Investing in your future".

CRediT authorship contribution statement

Eva Cañizares: Writing – review & editing, Writing – original draft, Investigation, Formal analysis, Conceptualization. **Juan Manuel Acién:** Writing – review & editing. **Berivan Özlem Gumuş:** Writing – review & editing. **Vicente Vives-Peris:** Writing – review & editing. **Miguel González-Guzmán:** Writing – review & editing, Writing – original draft, Supervision, Project administration, Investigation, Funding acquisition, Conceptualization. **Vicent Arbona:** Writing – review & editing, Writing – original draft, Supervision, Project administration, Methodology, Investigation, Funding acquisition, Conceptualization.

Declaration of competing interest

The authors declare no conflict of interest.

Data availability

Metabolomics data that support the findings of this study are openly available in Metabolights at www.ebi.ac.uk/metabolights/MTBLS8849, reference number MTBLS8849.

Acknowledgements

All metabolite profiling analyses were carried out at Universitat Jaume I central facilities (SCIC) under the inestimable help of Dr. Cristian Vicent.

Appendix A. Supplementary data

Supplementary data to this article can be found online at https://doi.org/10.1016/j.plaphy.2024.108483.

References

Acharya, P., Jayaprakasha, G.K., Crosby, K.M., Jifon, J.L., Patil, B.S., 2020. Nanoparticle-Mediated seed priming Improves germination, growth, yield, and quality of watermelons (Citrullus lanatus) at multi-locations in Texas. Sci. Rep. 10, 1–16. https://doi.org/10.1038/s41598-020-61696-7.

Ahuja, I., Kissen, R., Bones, A.M., 2012. Phytoalexins in defense against pathogens. Trends Plant Sci. 17, 73–90. https://doi.org/10.1016/j.tplants.2011.11.002.

Allwood, J.W., Ellis, D.I., Goodacre, R., 2008. Metabolomic technologies and their application to the study of plants and plant-host interactions. Physiol. Plantarum 132, 117–135. https://doi.org/10.1111/j.1399-3054.2007.01001.x.

Bak, S., Feyereisen, R., 2001. The involvement of two P450 enzymes, CYP83B1 and CYP83A1, in auxin homeostasis and glucosinolate biosynthesis. Plant Physiol. 127, 108–118. https://doi.org/10.1104/pp.127.1.108.

Bak, S., Nelsen, H.L., Halkier, B.A., 1998. The presence of CYP79 homologues in glucosinolate-producing plants shows evolutionary conservation of the enzymes in the conversion of amino acid to aldoxime in the biosynthesis of cyanogenic glucosides and glucosinolates. Plant Mol. Biol. 38, 725–734. https://doi.org/10.1023/A:1006064202774.

Bender, J., Fink, G.R., 1998. A Myb homologue, ATR1, activates tryptophan gene expression in Arabidopsis. Proc. Natl. Acad. Sci. U.S.A. 95, 5655–5660. https://doi.org/10.1073/pnas.95.10.5655.

Böttcher, C., von Roepenack-Lahaye, E., Schmidt, J., Schmotz, C., Neumann, S., Scheel, D., Clemens, S., 2008. Metabolome analysis of biosynthetic mutants reveals a diversity of metabolic changes and allows identification of a large number of new compounds in Arabidopsis. Plant Physiol. 147, 2107–2120. https://doi.org/10.1104/pp.108.117754.

Böttcher, C., Westphal, L., Schmotz, C., Prade, E., Scheel, D., Glawischnig, E., 2009. The multifunctional enzyme CYP71B15 (PHYTOALEXIN DEFICIENT3) converts cysteine-indole-3-acetonitrile to camalexin in the indole-3-acetonitrile metabolic network of Arabidopsis thaliana. Plant Cell 21, 1830–1845. https://doi.org/10.1105/tpc.109.066670.

Cao, H., Glazebrook, J., Clarke, J.D., Volko, S., Dong, X., 1997. The Arabidopsis NPR1 gene that controls systemic acquired resistance encodes a novel protein containing ankyrin repeats. Cell 88, 57–63. https://doi.org/10.1016/S0092-8674(00)81858-9.

Celenza, J.L., Quiel, J.A., Smolen, G.A., Merrikh, H., Silvestro, A.R., Normanly, J., Bender, J., 2005. The arabidopsis ATR1 Myb transcription factor controls indolic glucosinolate homeostasis. Plant Physiol. 137, 253–262. https://doi.org/10.1104/pp.104.054395.

Cessur, A., Albayrak, İ., Demirci, T., Göktürk Baydar, N., 2023. Silver and salicylic acid-chitosan nanoparticles alter indole alkaloid production and gene expression in root and shoot cultures of Isatis tinctoria and Isatis ermenekensis. Plant Physiol. Biochem. 202 https://doi.org/10.1016/j.plaphy.2023.107977.

Chambers, M.C., MacLean, B., Burke, R., Amodei, D., Ruderman, D.L., Neumann, S., Gatto, L., Fischer, B., Pratt, B., Egertson, J., Hoff, K., Kessner, D., Tasman, N., Shulman, N., Frewen, B., Baker, T.A., Brusniak, M.Y., Paulse, C., Creasy, D., Flashner, L., Kani, K., Moulding, C., Seymour, S.L., Nuwaysir, L.M., Lefebvre, B., Kuhlmann, F., Roark, J., Rainer, P., Detlev, S., Hemenway, T., Huhmer, A., Langridge, J., Connolly, B., Chadick, T., Holly, K., Eckels, J., Deutsch, E.W., Moritz, R.L., Katz, J.E., Agus, D.B., MacCoss, M., Tabb, D.L., Mallick, P., 2012. A cross-platform toolkit for mass spectrometry and proteomics. Nat. Biotechnol. 30, 918–920. https://doi.org/10.1038/nbt.2377.

Chini, A., Boter, M., Solano, R., 2009. Plant oxylipins: COI1/JAZs/MYC2 as the core jasmonic acid-signalling module. FEBS J. 276, 4682–4692. https://doi.org/10.1111/j.1742-4658.2009.07194.x.

De Ollas, C., Gonzalez-Guzman, M., Pitarch, Z., Matus, J.T., Candela, H., Rambla, J.L., Granell, A., Gomez-Cadenas, A., Arbona, V., 2021. Identification of ABA-mediated genetic and metabolic responses to soil flooding in tomato (Solanum lycopersicum L. Mill). Front. Plant Sci. 12 https://doi.org/10.3389/fpls.2021.613059.

Durango, D., Pulgarin, N., Echeverri, F., Escobar, G., Quiñones, W., 2013. Effect of salicylic acid and structurally related compounds in the accumulation of phytoalexins in cotyledons of common bean (Phaseolus vulgaris L.) cultivars. Molecules 18, 10609–10628. https://doi.org/10.3390/molecules180910609.

Ellis, C., Turner, J.G., 2002. A conditionally fertile coi1 allele indicates cross-talk between plant hormone signalling pathways in Arabidopsis thaliana seeds and young seedlings. Planta 215, 549–556. https://doi.org/10.1007/s00425-002-0787-4.

Erb, M., Kliebenstein, D.J., 2020. Plant Secondary Metabolites as Defenses, Regulators and Primary Metabolites - the Blurred Functional Trichotomy, pp. 1–26. https://doi.org/10.1104/pp.20.00433.

Feinbaum, R.L., Ausubel, F.M., 1992. Transcriptional regulation of the Arabidopsis thaliana chalcone synthase gene. Mol. Cell Biol. 8, 1985–1992.
Fernández-Calvo, P., Chini, A., Fernández-Barbero, G., Chico, J.-M., Gimenez-Ibanez, S., Geerinck, J., Eeckhout, D., Schweizer, F., Godoy, M., Franco-Zorrilla, J.M., Pauwels, L., Witters, E., Puga, M.I., Paz-Ares, J., Goossens, A., Reymond, P., De Jaeger, G., Solano, R., 2011. The Arabidopsis bHLH transcription factors MYC3 and MYC4 are targets of JAZ repressors and act additively with MYC2 in the activation of jasmonate responses. Plant Cell 23, 701–715. https://doi.org/10.1105/tpc.110.080788.
Frerigmann, H., Gigolashvili, T., 2014. MYB34, MYB51, and MYB122 distinctly regulate indolic glucosinolate biosynthesis in arabidopsis Thaliana. Mol. Plant 7, 814–828. https://doi.org/10.1093/mp/ssu004.
Frerigmann, H., Hoecker, U., Gigolashvili, T., 2021. New insights on the regulation of glucosinolate biosynthesis via COP1 and DELLA proteins in arabidopsis thaliana. Front. Plant Sci. 12, 1–15. https://doi.org/10.3389/fpls.2021.680255.
Frerigmann, H., Pislewska-Bednarek, M., Sánchez-Vallet, A., Molina, A., Glawischnig, E., Gigolashvili, T., Bednarek, P., 2016. Regulation of pathogen-triggered tryptophan metabolism in Arabidopsis thaliana by MYB transcription factors and indole glucosinolate conversion products. Mol. Plant 9, 682–695. https://doi.org/10.1016/j.molp.2016.01.006.
Gao, Y.Q., Jimenez-Sandoval, P., Tiwari, S., Stolz, S., Wang, J., Glauser, G., Santiago, J., Farmer, E.E., 2023. Ricca's factors as mobile proteinaceous effectors of electrical signaling. Cell 186, 1337–1351.e20. https://doi.org/10.1016/j.cell.2023.02.006.
Gigolashvili, T., Berger, B., Mock, H.-P., Müller, C., Weisshaar, B., Flügge, U.-I., 2007. The transcription factor HIG1/MYB51 regulates indolic glucosinolate biosynthesis in Arabidopsis thaliana. Plant J. 50, 886–901. https://doi.org/10.1111/j.1365-313X.2007.03099.x.
Glawischnig, E., Hansen, B.G., Olsen, C.E., Halkier, B.A., 2004. Camalexin is synthesized from indole-3-acetaldoxime, a key branching point between primary and secondary metabolism in Arabidopsis. Proc. Natl. Acad. Sci. U.S.A. 101, 8245–8250. https://doi.org/10.1073/pnas.0305876101.
González-García, Y., Cadenas-Pliego, G., Benavides-Mendoza, A., Juárez-Maldonado, A., 2023. Nanomaterials as novel elicitors of plant secondary metabolites. In: Nanotechnology in Agriculture and Agroecosystems. Elsevier, pp. 113–139. https://doi.org/10.1016/B978-0-323-99446-0.00016-7.
Grubb, C.D., Abel, S., 2006. Glucosinolate metabolism and its control. Trends Plant Sci. 11, 89–100. https://doi.org/10.1016/j.tplants.2005.12.006.
Hyde, C.L., Phillips, G.C., 1996. Silver nitrate promotes shoot development and plant regeneration of Chile pepper (Capsicum annuum L.) via organogenesis. Vitro Cell Dev. Biol. 32, 72–80.
Jogawat, A., Yadav, B., Chhaya, Lakra, N., Singh, A.K., Narayan, O.P., 2021. Crosstalk between phytohormones and secondary metabolites in the drought stress tolerance of crop plants: a review. Physiol. Plantarum 1–27. https://doi.org/10.1111/ppl.13328.
Khan, I., Raza, M.A., Awan, S.A., Shah, G.A., Rizwan, M., Ali, B., Tariq, R., Hassan, M.J., Alyemeni, M.N., Brestic, M., Zhang, X., Ali, S., Huang, L., 2020. Amelioration of salt induced toxicity in pearl millet by seed priming with silver nanoparticles (AgNPs): the oxidative damage, antioxidant enzymes and ions uptake are major determinants of salt tolerant capacity. Plant Physiol. Biochem. 156, 221–232. https://doi.org/10.1016/j.plaphy.2020.09.018.
Kim, J.H., Lee, B.W., Schroeder, F.C., Jander, G., 2008. Identification of indole glucosinolate breakdown products with antifeedant effects on Myzus persicae (green peach aphid). Plant J. 54, 1015–1026. https://doi.org/10.1111/j.1365-313X.2008.03476.x.
Kliebenstein, D.J., Figuth, A., Mitchell-Olds, T., 2002. Genetic architecture of plastic methyl jasmonate responses in Arabidopsis thaliana. Genetics 161, 1685–1696. https://doi.org/10.1093/genetics/161.4.1685.
Kranz, H.D., Denekamp, M., Greco, R., Jin, H., Leyva, A., Meissner, R.C., Petroni, K., Urzainqui, A., Bevan, M., Martin, C., Smeekens, S., Tonelli, C., Paz-Ares, J., Weisshaar, B., 1998. Towards functional characterisation of the members of the R2R3-MYB gene family from Arabidopsis thaliana. Plant J. 16, 263–276. https://doi.org/10.1046/j.1365-313X.1998.00278.x.
Kruszka, D., Sawikowska, A., Kamalabai Selvakesavan, R., Krajewski, P., Kachlicki, P., Franklin, G., 2020. Silver nanoparticles affect phenolic and phytoalexin composition of Arabidopsis thaliana. Sci. Total Environ. 716, 135361 https://doi.org/10.1016/j.scitotenv.2019.135361.
Kubasek, W.L., Shirley, B.W., McKillop, A., Goodman, H.M., Briggs, W., Ausubel, F.M., 1992. Regulation of flavonoid biosynthetic genes in germinating Arabidopsis seedlings. Plant Cell 4, 1229–1236. https://doi.org/10.2307/3869409.
Kuhl, C., Tautenhahn, R., Böttcher, C., Larson, T.R., Neumann, S., 2012. CAMERA: an integrated strategy for compound spectra extraction and annotation of liquid chromatography/mass spectrometry data sets. Anal. Chem. 84, 283–289. https://doi.org/10.1021/ac202450g.
Lefevere, H., Bauters, L., Gheysen, G., 2020. Salicylic acid biosynthesis in plants. Front. Plant Sci. 11, 1–7. https://doi.org/10.3389/fpls.2020.00338.
Leon-Reyes, A., Van der Does, D., De Lange, E.S., Delker, C., Wasternack, C., Van Wees, S. C.M., Ritsema, T., Pieterse, C.M.J., 2010. Salicylate-mediated suppression of jasmonate-responsive gene expression in Arabidopsis is targeted downstream of the jasmonate biosynthesis pathway. Planta 232, 1423–1432. https://doi.org/10.1007/s00425-010-1265-z.
Liu, J., Osbourn, A., Ma, P., 2015. MYB transcription factors as regulators of phenylpropanoid metabolism in plants. Mol. Plant 8, 689–708. https://doi.org/10.1016/j.molp.2015.03.012.
Liu, Z., Wang, H., Lv, J., Luo, S., Hu, L., Wang, J., Li, L., Zhang, G., Xie, J., Yu, J., 2022. Effects of plant hormones, metal ions, salinity, sugar, and chemicals pollution on glucosinolate biosynthesis in cruciferous plant. Front. Plant Sci. 13 https://doi.org/10.3389/fpls.2022.856442.
Moesta, P., Grisebach, H., 1980. Effects of biotic and abiotic elicitors on phytoalexin metabolism in soybean. Nature 286, 710–711. https://doi.org/10.1038/286710a0.
Naik, J., Tyagi, S., Rajput, R., Kumar, P., Pucker, B., Bisht, N., Misra, P., Stracke, R., Pandey, A.K., 2023. Flavonols have opposite effects on the interrelated glucosinolate and camalexin biosynthetic pathways in Arabidopsis thaliana. J. Exp. Bot. 0 https://doi.org/10.1093/jxb/erad391, 000.
Nakabayashi, R., Yonekura-Sakakibara, K., Urano, K., Suzuki, M., Yamada, Y., Nishizawa, T., Matsuda, F., Kojima, M., Sakakibara, H., Shinozaki, K., Michael, A.J., Tohge, T., Yamazaki, M., Saito, K., 2014. Enhancement of oxidative and drought tolerance in Arabidopsis by overaccumulation of antioxidant flavonoids. Plant J. 77, 367–379. https://doi.org/10.1111/tpj.12388.
Payne, G., Parks, T.D., Burkhart, W., Dincher, S., Ahl, P., Metraux, J.P., Ryals, J., 1988. Isolation of the genomic clone for pathogenesis-related protein 1a from Nicotiana tabacum cv. Xanthi-nc. Plant Mol. Biol. 11, 89–94. https://doi.org/10.1007/BF00015662.
Penninckx, A.M.A., Eggermont, K., Terras, F.R.G., Bart, P., 1996. Pathogen-Induced systemic activation of a plant defensin gene in arabidopsis follows a salicylic acid-Independent pathway. Plant Cell 8, 2309–2323.
Pfaffl, M.W., 2002. Relative expression software tool (REST(C)) for group-wise comparison and statistical analysis of relative expression results in real-time PCR. Nucleic Acids Res. 30 https://doi.org/10.1093/nar/30.9.e36, 36e – 36.
Pré, M., Atallah, M., Champion, A., De Vos, M., Pieterse, C.M.J., Memelink, J., 2008. The AP2/ERF domain transcription factor ORA59 integrates jasmonic acid and ethylene signals in plant defense. Plant Physiol. 147, 1347–1357. https://doi.org/10.1104/pp.108.117523.
Schreiner, M., Krumbein, A., Knorr, D., Smetanska, I., 2011. Enhanced glucosinolates in root exudates of brassica rapa ssp. rapa mediated by salicylic acid and methyl jasmonate. J. Agric. Food Chem. 59, 1400–1405. https://doi.org/10.1021/jf103585s.
Schuhegger, R., Nafisi, M., Mansourova, M., Petersen, B.L., Olsen, C.E., Svatos, A., Halkier, B.A., Glawischnig, E., 2006. CYP71B15 (PAD3) catalyzes the final step in camalexin biosynthesis. Plant Physiol. 141, 1248–1254. https://doi.org/10.1104/pp.106.082024.
Silva-Navas, J., Moreno-Risueno, M.A., Manzano, C., Téllez-Robledo, B., Navarro-Neila, S., Carrasco, V., Pollmann, S., Gallego, F.J., Juan, C., 2016. Flavonols mediate root phototropism and growth through regulation of proliferation-to-differentiation transition. Plant Cell 28, 1372–1387. https://doi.org/10.1105/tpc.15.00857.
Smith, C. a, Want, E.J., O'Maille, G., Abagyan, R., Siuzdak, G., 2006. XCMS: processing mass spectrometry data for metabolite profiling using nonlinear peak alignment, matching, and identification. Anal. Chem. 78, 779–787. https://doi.org/10.1021/ac051437y.
Sønderby, I.E., Hansen, B.G., Bjarnholt, N., Ticconi, C., Halkier, B.A., Kliebenstein, D.J., 2007. A systems biology approach identifies a R2R3 MYB gene subfamily with distinct and overlapping functions in regulation of aliphatic glucosinolates. PLoS One 2, e1322. https://doi.org/10.1371/journal.pone.0001322.
Utsugi, S., Sakamoto, W., Murata, M., Motoyoshi, F., 1998. Arabidopsis thaliana vegetative storage protein (VSP) genes: gene organization and tissue-specific expression. Plant Mol. Biol. 38, 565–576. https://doi.org/10.1023/A:1006072014605.
Van der Does, D., Leon-Reyes, A., Koornneef, A., Van Verk, M.C., Rodenburg, N., Pauwels, L., Goossens, A., Körbes, A.P., Memelink, J., Ritsema, T., Van Wees, S.C.M., Pietersea, C.M.J., 2013. Salicylic acid suppresses jasmonic acid signaling downstream of SCFCOI1-JAZ by targeting GCC promoter motifs via transcription factor ORA59. Plant Cell 25, 744–761. https://doi.org/10.1105/tpc.112.108548.
Venegas-Molina, J., Proietti, S., Pollier, J., Orozco-Freire, W., Ramirez-Villacis, D., Leon-Reyes, A., 2020. Induced tolerance to abiotic and biotic stresses of broccoli and Arabidopsis after treatment with elicitor molecules. Sci. Rep. 10, 1–17. https://doi.org/10.1038/s41598-020-67074-7.
Venkatachalam, P., Jinu, U., Gomathi, M., Mahendran, D., Ahmad, N., Geetha, N., Sahi, S.V., 2017. Role of silver nitrate in plant regeneration from cotyledonary nodal segment explants of Prosopis cineraria (L.) Druce.: a recalcitrant medicinal leguminous tree. Biocatal. Agric. Biotechnol. 12, 286–291. https://doi.org/10.1016/j.bcab.2017.10.017.
Vishwakarma, K., Shweta, Upadhyay, N., Singh, J., Liu, S., Singh, V.P., Prasad, S.M., Chauhan, D.K., Tripathi, D.K., Sharma, S., 2017. Differential phytotoxic impact of plant mediated silver nanoparticles (AgNPs) and silver nitrate (AgNO3) on Brassica sp. Front. Plant Sci. 8, 1–12. https://doi.org/10.3389/fpls.2017.01501.
Wanner, L.A., Li, G., Ware, D., Somssich, I.E., Davis, K.R., 1995. The phenylalanine ammonia-lyase gene family in Arabidopsis thaliana. Plant Mol. Biol. 27, 327–338. https://doi.org/10.1007/BF00020187.
Wasternack, C., 2007. Jasmonates: an update on biosynthesis, signal transduction and action in plant stress response, growth and development. Ann. Bot. 100, 681–697. https://doi.org/10.1093/aob/mcm079.
Wei, J., Fang, Y., Jiang, H., Wu, X., Zuo, J., Xia, X., Li, J., Stich, B., Cao, H., Liu, Y., 2022. Combining QTL mapping and gene co-expression network analysis for prediction of candidate genes and molecular network related to yield in wheat. BMC Plant Biol. 22, 1–14. https://doi.org/10.1186/s12870-022-03677-8.
Widemann, E., Bruinsma, K., Walshe-Roussel, B., Rioja, C., Arbona, V., Saha, R.K., Letwin, D., Zhurov, V., Gomez-Cadenas, A., Bernards, M.A., Grbic, M., Grbic, V., 2021. Multiple indole glucosinolates and myrosinases defend Arabidopsis against Tetranychus urticae herbivory. Plant Physiol. 187, 116–132. https://doi.org/10.1093/plphys/kiab247.
Wiesner, M., Hanschen, F.S., Schreiner, M., Glatt, H., Zrenner, R., 2013. Induced production of 1-methoxy-indol-3-ylmethyl glucosinolate by jasmonic acid and

methyl jasmonate in sprouts and leaves of pak choi (Brassica rapa ssp. chinensis). Int. J. Mol. Sci. 14, 14996–15016. https://doi.org/10.3390/ijms140714996.

Yi, S.Y., Lee, M., Park, S.K., Lu, L., Lee, G., Kim, S.G., Kang, S.Y., Lim, Y.P., 2022. Jasmonate regulates plant resistance to Pectobacterium brasiliense by inducing indole glucosinolate biosynthesis. Front. Plant Sci. 13, 1–20. https://doi.org/10.3389/fpls.2022.964092.

Yoshikawa, M., 1978. Diverse modes of action of biotic and abiotic phytoalexin elicitors [19]. Nature 275, 546–547. https://doi.org/10.1038/275546a0.

Zang, Y., Zheng, W., He, Y., Hong, S.B., Zhu, Z., 2015. Global analysis of transcriptional response of Chinese cabbage to methyl jasmonate reveals JA signaling on enhancement of secondary metabolism pathways. Sci. Hortic. 189, 159–167. https://doi.org/10.1016/j.scienta.2015.04.008.

Zarate, S.I., Kempema, L. a, Walling, L.L., 2007. Silverleaf whitefly induces salicylic acid defenses and suppresses effectual jasmonic acid defenses. Plant Physiol. 143, 866–875. https://doi.org/10.1104/pp.106.090035.

Zhang, N., Zhou, S., Yang, D., Fan, Z., 2020. Revealing shared and distinct genes responding to JA and SA signaling in arabidopsis by meta-analysis. Front. Plant Sci. 11, 1–17. https://doi.org/10.3389/fpls.2020.00908.

Zhao, Y., Hull, A.K., Gupta, N.R., Goss, K.A., Alonso, J., Ecker, J.R., Normanly, J., Chory, J., Celenza, J.L., 2002. Trp-dependent auxin biosynthesis in Arabidopsis: involvement of cytochrome P450s CYP79B2 and CYP79B3. Genes Dev. 16, 3100–3112. https://doi.org/10.1101/gad.1035402.

Zhurov, V., Navarro, M., Bruinsma, K. a, Arbona, V., Santamaria, M.E., Cazaux, M., Wybouw, N., Osborne, E.J., Ens, C., Rioja, C., Vermeirssen, V., Rubio-Somoza, I., Krishna, P., Diaz, I., Schmid, M., Gómez-Cadenas, A., Van de Peer, Y., Grbic, M., Clark, R.M., Van Leeuwen, T., Grbic, V., 2014. Reciprocal responses in the interaction between arabidopsis and the cell-content-feeding chelicerate herbivore spider mite. Plant Physiol. 164, 384–399. https://doi.org/10.1104/pp.113.231555.